Journal of Materials Research and Technology 36 (2025) 6994–7007

Contents lists available at ScienceDirect

Journal of Materials Research and Technology

journal homepage: www.elsevier.com/locate/jmrt

Kinetic of copper powders production via galvanic deposition on carbon steel activated by high energy ball-milling

Alvaro Soliz [a,*], Pia Rojas [a], Danny Guzman [a,**], Luis Cáceres [b], Felipe M. Galleguillos-Madrid [c], Norman Toro [d], Freddy Celis [e]

[a] Departamento de Ingeniería en Metalurgia, Facultad de Ingeniería, Universidad de Atacama, Av. Copayapu 485, Copiapó, 1530000, Chile
[b] Departamento de Ingeniería Química y Procesos de Minerales, Universidad de Antofagasta, Av. Universidad de Antofagasta 02800, Antofagasta, 1271155, Chile
[c] Centro de Desarrollo Energético Antofagasta, Universidad de Antofagasta, Antofagasta, 1240000, Chile
[d] Faculty of Engineering and Architecture, Universidad Arturo Prat, Iquique, 1110939, Chile
[e] Laboratorio de Procesos Fotónicos y Electroquímicos, Facultad de Ciencias Naturales y Exactas, Universidad de Playa Ancha, Valparaíso, Chile

ARTICLE INFO

Handling Editor: P Rios

Keywords:
Carbon steel
Copper powders
Ball-milling
Galvanic process

ABSTRACT

Understanding the kinetics of high-purity zero-valent copper production via galvanic displacement process has crucial implications for numerous industrial applications and the development of new cost-effective technologies. This study presents a novel approach to galvanic copper deposition using carbon steel chips and powders as reducing agents. The effects of milling time, used to prepare activated carbon steel powders via high-energy ball milling, and solution acidity on the kinetics and morphological attributes of the deposited copper were investigated. Notably, the galvanic process exhibited a significant dependency of the copper and iron reaction kinetics on both the initial state of the carbon steel (chips or powders) and the acidity of the solution, which was also influenced by the hydrogen evolution reaction as secondary reaction. The most favorable conditions for galvanic deposition were achieved employing carbon steel powders in acidic solutions, enabling rapid copper deposition in less than 5 min, with purities ranging between 90 and 94 %. In contrast, carbon steel chips required reaction times longer than 30 min. Meanwhile, the copper galvanic deposition was not completely evident in solution of natural acidity by using carbon steel powders, due to the formation of a passivating barrier on the carbon steel surface. Experimental results indicated that the reaction rate follows a global second-order kinetics. Scanning electron microscopy, X-ray diffraction, and Raman spectroscopy analysis corroborated the results.

1. Introduction

Currently, various technologies are available for the production of high-purity zero-valent copper powders from synthetic and industrial solutions. The efficiency and viability of these processes depend strongly on a detailed understanding of the numerous factors that influence the reaction kinetics, which is fundamental for the strategic selection and development of high-performance methodologies aimed at achieving highly efficient processes. Among these technologies, electrolysis [1–4], galvanic displacement or cementation [5–9], chemical reduction [10–13], green synthesis and biosynthesis [14–17] stand out, each with its own advantages and limitations, focusing on specific areas of interest. Through a comparative analysis we can indicate that chemical reduction involves high operational costs, primarily due to the use of expensive and, in many cases, toxic chemical reagents such as ascorbic acid, sodium borohydride, polyvinylpyrrolidone, hydrazine, sodium hypophosphite and other. These substances not only increase the cost of the process but also pose significant risks to human health and the environment. These drawbacks have driven the search for more sustainable alternatives, such as the use of green reductants. However, these also present limitations associated with variability in their composition, which can affect process reproducibility, and limitations during industrial installations. On the other hand, while electrolysis enables the production of copper powders with purities exceeding 99 %, this process generally requires high current densities, that are higher than 600 A/m^2, which significantly increases both energy consumption and capital costs by installing specialized electrolysis cells. In particular, the galvanic displacement methodology is an inexpensive and straightforward

* Corresponding author.
** Corresponding author.
E-mail addresses: alvaro.soliz@uda.cl (A. Soliz), danny.guzman@uda.cl (D. Guzman).

https://doi.org/10.1016/j.jmrt.2025.04.300
Received 29 January 2025; Received in revised form 24 April 2025; Accepted 28 April 2025
Available online 30 April 2025
2238-7854/© 2025 The Authors. Published by Elsevier B.V. This is an open access article under the CC BY license (http://creativecommons.org/licenses/by/4.0/).

alternative for synthesizing zero-valent metals. Its principle is based on the electrochemical potential difference between a less noble metal and the metal ion of a more noble metal. This galvanic displacement is a spontaneous electrochemical reaction that occurs at the solid-liquid interface, promoting the oxidation of the less noble metal and the reduction of the ion of the more noble metal to its metallic form. A well-known example is copper deposition on iron, as demonstrated by the following partial and global reactions:

$$\text{Anodic reaction}: Fe \rightarrow Fe^{+2} + 2e^{-} \quad (1)$$

$$\text{Cathodic reaction}: Cu^{+2} + 2e^{-} \rightarrow Cu \quad (2)$$

$$\text{Global reaction}: Cu^{+2} + Fe \rightarrow Cu + Fe^{+2} \quad (3)$$

For copper, typical metals such as iron, zinc, aluminum, and magnesium are widely used as reducing agents, where the reaction kinetics can be studied under multiple conditions [18–21]. Comparative galvanic studies of copper production using iron provide valuable insights into the main factors that affect copper deposition kinetics, such as initial copper concentration, temperature, hydrodynamic behavior, cell design, solution pH, and others. These studies serve as models to explore alternatives for faster production of high-grade copper [5, 22–26]. The variation of these factors can accelerate or decelerate the reaction kinetics, having multiple impacts on metal production. In recent years, various kinetic models have been developed to describe galvanic copper deposition, showing reactions of first or second order kinetics with respect to copper [5,6,27,28].

Mechanical milling is a dry grinding process that primarily increases material reactivity and the uniformity of spatial distribution of elements. In this process, high strain is introduced from multiple directions into the powder material, inducing high-energy impacts from collisions between the grinding medium and particles, causing severe plastic deformation [29]. Two key mechanisms are involved in the mechanical milling process, focusing on material activation: (i) an increase in the active surface area of the powders due to a reduction in material size, and (ii) a rise in internal energy caused by the generation of microstructural defects. Studies of galvanic copper cementation using different reducing agents, mechanically activated by high-energy ball milling, provide novel alternatives for the mass production of copper. The use of aluminum powders have shown a shortening of the initial slow-rate period for copper cementation and an alteration in the rate-controlling mechanism of the reaction, with a recovery of nearly 25 % at 25 °C after 4 min of reaction [7]. Similar changes on a rapid kinetic of copper cementation were observed by using iron powders mechanically activated where copper particles sizes between 180 nm and 46 μm after 12 min of reaction were founded [6]. On the other hand, studies shown that by using zinc dust milled during 2 h reaching a −300 mesh size, an enhancement in copper cementation was founded using 300 % excess zinc dust with reaction times from 2 min [30]. Additionally, studies employing aluminum as a reducing agent have revealed that the primary limitation in galvanic copper deposition in acid media is the presence of a protective oxide/hydroxide layer on the aluminum surface, which slows down the electrochemical reactions and reduce the effectiveness of the Al|Cu redox couple. This phenomenon arise because the passive layer on aluminum dissolves faster and efficient under alkaline rather than acidic conditions [8,31]. On the other hand, the use of zinc powders presents key challenges associated to their high sensitivity to dissolved oxygen and hydrogen protons in solution, where competing reactions such as oxygen reduction and hydrogen evolution can substantially increase zinc consumption beyond stoichiometry [8, 30].

This study aims to identify sustainable alternatives that facilitate the adoption of low-capital solution, particularly for implementation in small and medium-scale mining operations, by taking advantages of existing infrastructure. In this context, carbon steel is a widely used material due to its high iron content, which enables its use as a reducing agent in copper production within the mining-metallurgical industry. Moreover, this material exhibit high circularity, as its scrap can be efficiently recycled and remelted to produce new steel, further enhancing its environmental and economic value. Building upon these characteristics, the novelty of this study lies in the exploration of carbon steel powders as a more sustainable and efficient alternative for copper deposition via galvanic process, particularly when compared to other commonly used metals such as aluminum and zinc. In this context, we report the direct synthesis of zero-valent copper powders via a galvanic displacement process using carbon steel powders prepared by high-energy ball milling. A novel analysis was conducted on the influence of the milling time of carbon steel chips and the solution acidity on copper production. Furthermore, an extended kinetic model to describe copper kinetics in terms of copper and iron ions was developed. The results were complemented by scanning electron microscopy (SEM) coupled with energy-dispersive X-ray, X-ray diffraction (XRD), Raman spectroscopy, and microstructural analysis using the Rietveld method, providing new insights into the galvanic copper deposition process and the role of carbon steel powders as a effectively reducing agent in copper cementation processes.

2. Materials and methods

2.1. Material preparation

AISI 1020 carbon steel, with nominal chemical composition of (wt. %): 0.18–0.23C, 0.3–0.6 Mn, 0.1–0.35 Si, ≤0.04 P, ≤0.05 S, and traces of Cu, Cr, and Fe as the balance, was used in this study as reducing agent in two different initial forms. The first form was chips, prepared through a continuous cutting process on a mechanical lathe (Sumore SP2123–I, Sumore Machinery, Shanghai, China), resulting in small samples with a spiral appearance. The second form was powders, prepared by high-energy ball milling of the chips for durations of 10, 15 and 20 h. The milling process was performed using a planetary ball miller (Retsch-PM100, Retsch GmbH, Haan, Germany), following the optimized procedure reported in our previous work [32]. The process was conducted under a vacuum atmosphere, and 1 % stearic acid was added as a control agent to minimize particle agglomeration. After preparation, the carbon steel samples were stored in a desiccator until their use in the subsequent galvanic deposition process. Preliminary studies were done considering a whole spectrum of milling time for carbon steel chip which includes millings during 1, 2 and 5 h. This approach was performed in order to understand the milling time influence on the copper grade after galvanic process.

The tests solutions were prepared using copper (II) sulfate pentahydrate as the precursor salt and deionized water. No additional oxygen purge was performed. A fix initial concentration of 3.75 g/L Cu^{+2} was maintained in all solutions, while the acidity was varied by adding H_2SO_4 to reach concentrations of 4.7 and 9.4 g/L, along with a solution of natural acidity (0.0 g/L H_2SO_4 with a natural pH of 4.48). All chemicals used were of analytical-grade reagent quality (Merck S.A.).

2.2. Galvanic deposition process

The galvanic deposition process was carried out at room temperature of 21 ± 0.2 °C in a 250 mL stirred batch reactor equipped with baffles to improve flow patterns and enhance solid-liquid contact. A stoichiometric molar ratio of 1:1 between copper and iron was used in all experiments, according to the reaction in Equation (3). The weight of carbon steel was calculated considering the iron content in the alloy. The process was conducted at 2200 rpm, and 0.5 mL solution samples were withdrawn at specific reaction times of 0.25, 0.5, 1, 1.5, 2, 4, 8, 15, 20 and 30 min for chemical analysis of total copper (CuT) and total iron (FeT) ion concentrations using atomic absorption spectroscopy (SavantAA, GBC, Braeside, VIC, Australia).

After the copper deposition process, the slurry was filtered through

Whatman No. 1 filter paper using a vacuum pump connected to a Büchner funnel. Subsequently, the copper powders were washed with deionized water, rinsed with isopropyl alcohol, and dried at 60 °C in a hot air oven (UN75, Memmert, Schwabach, Germany). The copper grade of the deposited powders was analyzed, prior to a digestion step, using atomic absorption spectroscopy. The copper reduction efficiency was determined according to the follow equation:

$$\eta = \frac{C_{0,Cu} - C_{Cu}}{C_{0,Cu}} \quad (4)$$

where, $C_{0,Cu}$ and C_{Cu} are the initial and final copper ion concentration after a defined reaction time.

2.3. Characterization

Surface characterization was conducted using scanning electron microscopy (Zeiss EVO MA 10, Zeiss, Oberkochen, Germany) equipped with an energy-dispersive X-ray (EDS) analyzer. The particle size distribution was measured by laser scattering (Malvern Mastersize 2000, Malvern Panalytical, Westborough, MA, USA). Identification of the main phases was performed using X-ray diffraction (XRD) (Shimadzu XRD-600, Shimadzu Corp., Kyoto, Japan) with an angular step of 0.02° (2θ) and a counting time of 4 s per step, utilizing Cu Kα radiation. XRD patterns were analyzed by using the Rietveld method [33] in the Materials Analysis Using Diffraction (MAUD) program [34]. The Raman spectra of the samples were acquired by using a microRaman system Oxford Instrument WITec model alpha300R equipped with a 532 nm laser line and the CCD camera cooler by a Peltier at −65 °C. The laser power was set at less than 5 % to avoid any burn of the sample and the integration time was 10s per spectrum.

2.4. Open circuit potential measurements

The open circuit potential (OCP) tests was conducted using a potentiostat/galvanostat BioLogic VSP-300 (BioLogic, Seyssinet-Pariset, France) and a three-electrode cell system. A modify carbon paste electrode was used as working electrode, a spiral platinum wire was used as the counter electrode, and an Ag/AgCl electrode as the reference electrode. The working electrode was prepared by mixing 1.2 g of carbon steel powders (obtained at the different milling times), 0.6 g of graphite powder, and 0.6 g of mineral oil to obtain the a homogeneous paste. This paste was tightly packed into a plastic PVC bar with adequate perforations to obtain the electrical contact through a stainless steel bar. The OCP measurements were performed at room temperature in solution of natural acidity (0 g/L H_2SO_4) and in solution with 4.7 g/L H_2SO_4. All the potentials reported in this work refer to the standard hydrogen electrode (SHE).

3. Results and discussion

To understand the behavior of high-purity copper production as influenced by the ball milling time of carbon steel chips, previous studies have examined milling durations ranging from 1 to 5 h. The morphological analysis of carbon steel after these milling times revealed the formation of large flake-like particles, which exhibit a slight decrease in size with increasing milling time (see Fig. S1 in the Supporting Information). When this carbon steel particles were used in the copper deposition process, copper was found to deposit uniformly across the steel surface, maintaining morphological patterns similar to those of the original steel particles (see Fig. S2 in the Supporting Information). However, chemical analysis of the final product indicated low copper content, with purities levels ranging from 65 to 70 %, with iron comprising the remainder. This results implies that the carbon steel was encapsulated by a copper film, limiting a continuous galvanic process of Fe|Cu couple. Additionally, XRD analysis confirms a α-ferrite phase in the carbon steel particles after milling, as well as the formation of a pure copper phase and some copper oxides after the copper deposition process (see Fig. S3 in the Supporting Information). Therefore, in the follow sections, we present the main results for carbon steel milling times longer than 5 h, which enabled to production of copper powders with significantly higher purity.

3.1. Morphological and microstructural patters of carbon steel

Fig. 1 shows SEM images of carbon steel chips and carbon steel powders obtained from the cutting and milling process, respectively. Comparing the morphological patterns, the carbon steel chips (Fig. 1a) exhibit a spiral shape with average radius of 2 mm, a length of 10 mm, and a thickness of 1 mm. This spiral shape is attributed to the plastic deformation caused by the cutting process. Whereas, the carbon steel powders obtained after 10, 15, and 20 h of milling (Fig. 1b–d) exhibit particles with irregular edges and a heterogeneous particle size distribution, consisting mainly of individual particles and agglomerates in the form of flakes. However, these results shows a clear trend of decreasing particle and agglomerate sizes with milling time, resulting in D50 values of 15.50, 9.04, and 7.54 μm, and D90 values of 53.48, 42.58, and 37.86 μm for milling times of 10, 15, and 20 h, respectively.

The microstructural changes of carbon steel powders obtained from milling were characterized by XRD analysis, as shown in Fig. 2. The diffractograms analysis reveals the presence of well-known peaks associated to α-ferrite phase. By comparing the diffractograms at different milling times, the results show a slight decrease in peak intensity, leading to an increase in the full width-half maximum (FWHM) value as the milling process progress. These changes can be attributed to a decrease in crystallite size and an increase in lattice microstrains caused by plastic deformation during the milling process. The Rietveld method was then employed to analyze the microstructural parameters, including crystallite size, lattice microstrains, and lattice parameter, using the methodology described in our previous work [32]. The microstructural results reveal crystallite sizes of 17 ± 0.15, 13 ± 0.19 and 13.1 ± 0.02 nm and lattice microstrains of $4.1{\cdot}10^{-3}{\pm}4.55{\cdot}10^{-4}$, $6.3{\cdot}10^{-3}{\pm}1.42{\cdot}10^{-4}$ and $6.8{\cdot}10^{-3}{\pm}1.41{\cdot}10^{-4}$ for milling times of 10, 15 and 20 h, respectively. These findings indicate that the carbon steel has reached its comminution limit after 15 h of milling under vacuum conditions. Additionally, the lattice parameter values remained nearly unchanged with milling time, with values of $0.2869 \pm 8{\cdot}10^{-6}$, $0.2871 \pm 2{\cdot}10^{-5}$ and $0.2871 \pm 8{\cdot}10^{-6}$ nm for 10, 15 and 20 h of milling, respectively. These values are in close agreement with the theoretical lattice parameter for iron (0.2866 nm) [35] and those obtained in our previous work [32], indicating negligible expansion or contractions of the unit cell volume during the milling process of carbon steel chips.

3.2. Galvanic deposition of copper on carbon steel

3.2.1. Deposition process using carbon steel chips

Fig. 3 shows the time evolution of copper and iron ion concentrations during the galvanic copper deposition on carbon steel chips, considering tests solutions of natural acidity and those with additional sulfuric acid. From the results, similar trends are described, with an evident decrease in copper concentration and an increase in iron concentration over time for both tests solutions without and with sulfuric acid. According to the trends of copper and iron concentrations with time, the results show that the kinetics of copper deposition slightly increase with the acidity of the solution, principally during intermediate reaction times of 5–20 min. This is followed by a quasi-stationary condition at 30 min of reaction, where concentrations lower than 0.7 ppm for copper (Fig. 3a) and higher than 2.3 ppm for iron (Fig. 3b) were obtained. Using Equation (4), the maximum reduction efficiencies were approximately equals to 82, 84 and 86 % for the solutions with 0.0, 4.7 and 9.4 g/L H_2SO_4, respectively, at 30 min of reaction. These variations in reduction efficiencies can be explained by a synergistic effect associated with the

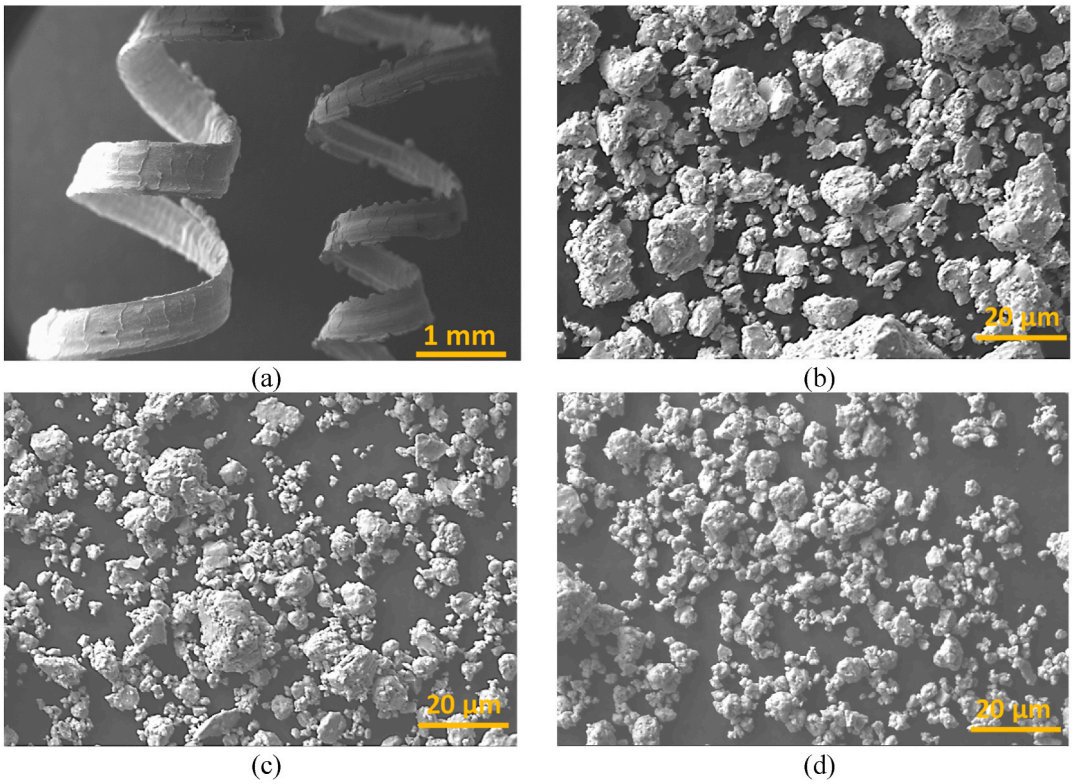


Fig. 1. SEM images of carbon steel chips (a) and carbon steel powders prepared during milling times of 10 h (b), 15 h (c), and 20 h (d).

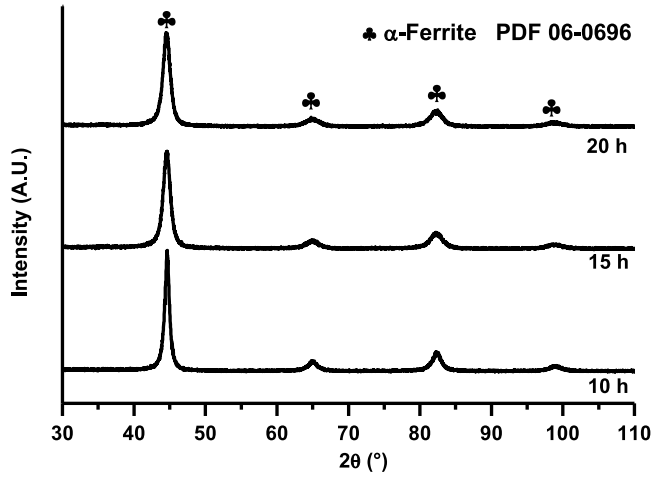


Fig. 2. XRD patterns of carbon steel powders prepared at milling times of 10, 15 and 20 h.

concentration of hydrogen protons and dissolved oxygen in the solution. In this context, competition between electrochemical couples of the oxygen reduction reaction and copper reduction reaction, as well as further iron oxidation, results in the formation of iron oxide-hydroxides deposited on the steel surface, forming a protective layer that limits the availability of active sites needed for iron oxidation. Additionally, this iron-oxygen couple is enhanced by the high hydrodynamic turbulence in the batch reactor, facilitating significant mass transfer of dissolved oxygen from the bulk solution to metallic steel surface [36]. This reaction competition can be extended during the first 2 min of reaction, where the copper and iron concentrations show similar trends for both test solutions. On the other hand, for reaction times longer than 2 min, the results show a rapid decrease in copper ion concentration with solution acidity. This changes can be attributed to an increases in hydrogen protons from the sulfuric acid, which promotes the dissolution of the previously formed protective oxide layer on the carbon steel surface, leaving new active sites for iron oxidation and copper reduction. These results are consistent with findings in literature [26,37,38], where increasing solution acidity promotes a higher galvanic deposition rate of copper on carbon steel chips, supported by the thermodynamic stability predicted by Pourbaix and solubility diagrams for iron [39–41]. In addition, the quantification of iron and copper content in the tests solutions indicates satisfactory reduction efficiencies (>80 %) for copper within times periods shorter than 30 min.

3.2.2. Deposition process using carbon steel powders

Fig. 4 compares the time evolution of copper and iron ion concentrations during the galvanic copper deposition using carbon steel powders prepared by milling for 10, 15 and 20 h. The figure also illustrates the influence of solution acidity at each milling time. The outcomes of this results reveals a notable influence of solution acidity on the temporal variations of copper and iron concentrations during the galvanic deposition process, which is also dependent on the duration of ball-milling applied to the steel chips. In general, the copper deposition process exhibits similar trends in the temporal variations of copper and iron ion concentration with milling time, especially in tests solutions containing sulfuric acid. Under these conditions, the copper concentration profile shows a rapid decrease during the first 5 min of the reaction, followed by a gradual linear increase at longer reaction times. Conversely, changes in iron concentration over time in solutions with sulfuric acid reveal a rapid increase during the first 5 min, which then remains constant at longer reaction times. In comparison, the profiles of copper and iron ion concentrations show a strong dependence on milling time when the galvanic process is carried out using a solution with natural acidity. Under that condition, using carbon steel powders prepared by 10 h of milling, the copper concentration continuously decreases over time, reaching a steady state at around 25 min (Fig. 4a). However, for carbon steel powders obtained during 15 (Fig. 4c) and 20 h

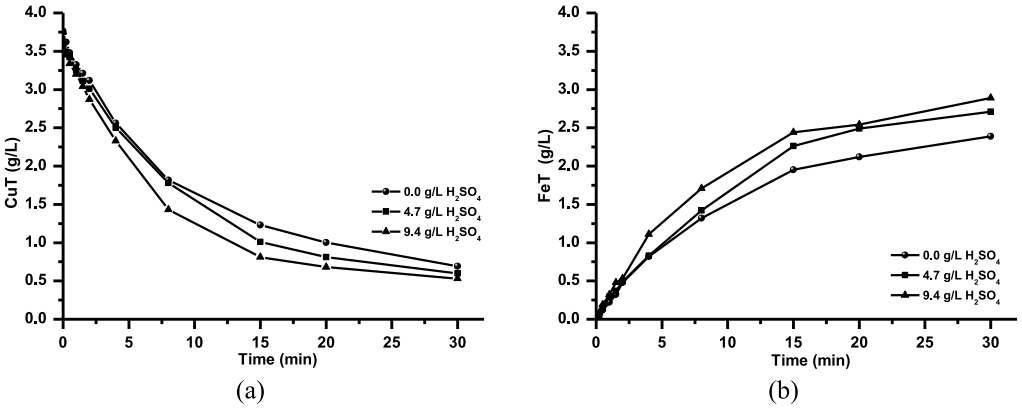


Fig. 3. Temporal evolution of copper ion (a) and iron ion (b) concentrations during galvanic deposition using carbon steel chips in solutions without and with additional sulfuric acid.

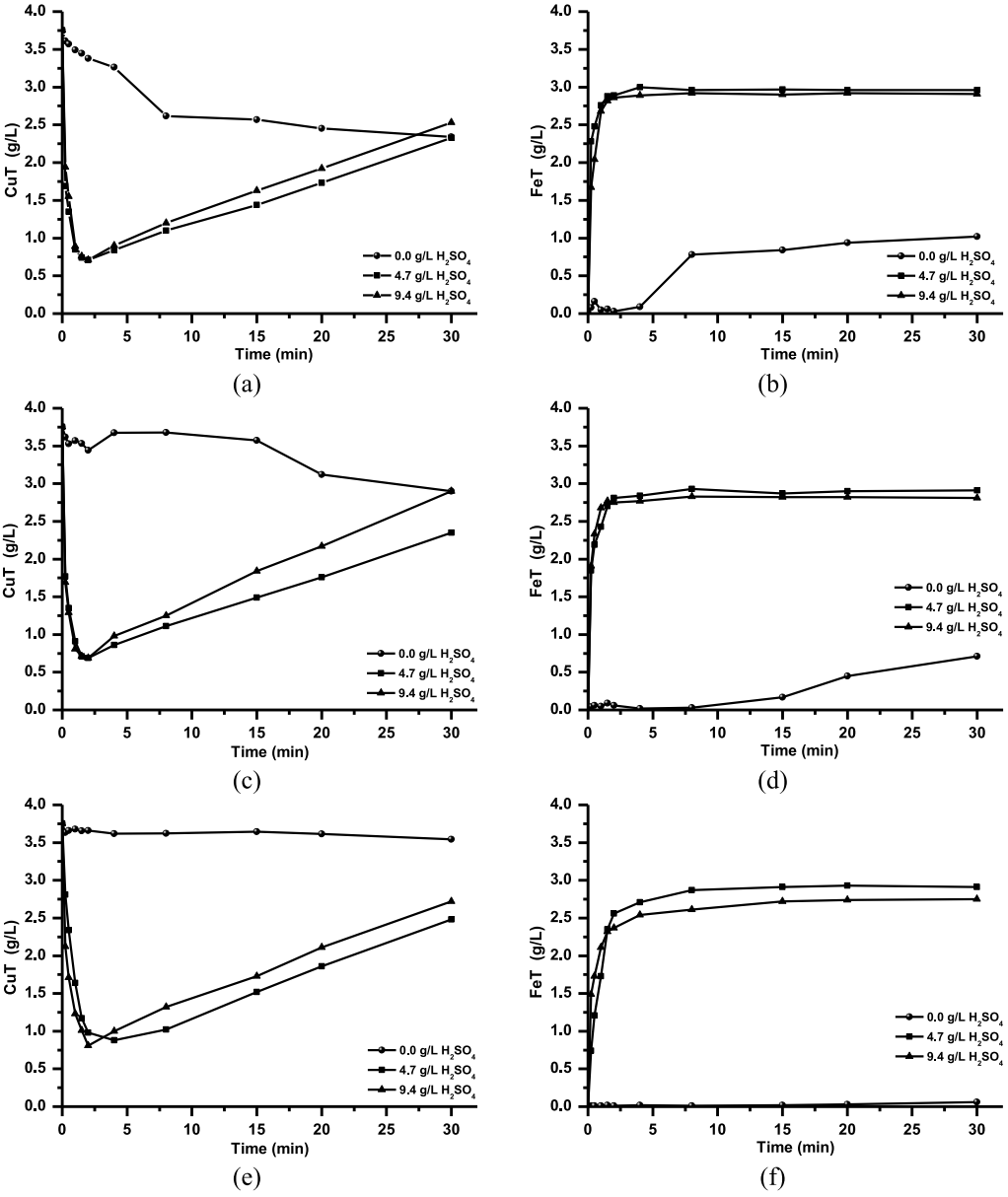


Fig. 4. Copper ion concentration (a, c, e), and iron concentration (b, d, f) variations during the galvanic deposition using carbon steel powders milled at 10 h (a, b), 15 h (c, d), and 20 h (e, f), in solutions without and with additional sulfuric acid.

(Fig. 4e) of milling, the copper ion concentration remains almost negligible over time, as evidenced by the lower variability, with copper concentrations close to the initial concentrations of 2.9 and 3.54 g/L respectively. These copper concentration profiles are consistent with the iron concentration profiles, according to Equation (3), revealing a continuous stopping in reaction as the milling time of carbon steel chips increases. These results indicates a complex relationship between the kinetics of galvanic copper deposition, the solution acidity, and the milling time of steel chips. In consequence, in solutions with natural acidity, the limited galvanic process involving copper reduction and iron oxidation reactions with milling time can be attributed to multiples factors: i) the high reactivity of the carbon steel powders due to milling process, which leads to changes in their microstructural parameters, as microstrains and crystallite size. This promotes fast iron oxidation, having the oxygen reduction reaction as the primary cathodic counter reaction and copper reduction as secondary reaction, resulting in the formation of a strong passive layer (composed of copper and iron oxides) that limits the availability of active sites for further iron oxidation reaction, ii) the formation of a barrier on individual carbon steel particles that covers the carbon steel samples limiting the active sites for the further iron oxidation, which can attributed to the formation of iron oxides/hydroxides or the encapsulation of carbon steel powder due to the copper deposited, and iii) a chemical and physical synergism between the copper reduction reaction and the hydrodynamic turbulence, which initially promotes turbulent agglomeration of fine carbon steel particles through the interaction and adhesion forces driven by hydrodynamic turbulence [42,43]. This competition between physical and chemical factors (turbulence, cathodic copper reduction, oxygen reduction reaction, solid barrier formation) in solutions with natural acidity (0.0 g/L H_2SO_4) limits the deposition rate of zero-valent copper particles, requiring longer contact times to complete the galvanic deposition process.

On the other hand, in the case of solutions with variable acidity (4.7 and 9.4 g/L H_2SO_4), the milling process revealed different behaviors in the temporal profiles for both copper and iron ions. For the iron oxidation reaction in the Fe|Cu couple, the temporal iron profile indicates that the reaction stopped after ~5 min of reaction, with no further significant changes in iron concentration, indicating the maximum consumption of iron. For the copper reduction reaction, the temporal copper profile indicates a reversible reaction, where during the first ~5 min zero-valent copper is obtained. However, for reaction times longer than ~5 min, the previously deposited metallic copper undergoes continuous oxidation up to 30 min of reaction. The absence of significant changes in iron concentration after ~5 min indicates that the steel is no longer participating in the overall reaction due to its incomplete consumption. As a result, the counter cathodic reaction is attributed to hydrogen evolution, driven by the Cu|H_2 couple and the high concentration of H^+ ions from sulfuric acid. This was confirmed by the significant hydrogen production in the batch reactor, where numerous bubbles were observed evolving from the process. Furthermore, at constant solution acidity, the results shows a slight slowly copper deposition as the milling time increases.

A comparison of the main results for galvanic copper deposition is presented in Table 1. The results show that the minimum concentration of copper ions using carbon steel chips ranged between 0.53 and 0.69 g/L, achieved after 30 min of reaction under all three conditions of solution acidity. Whereas, the minimum concentration of copper ions using carbon steel powders varied depending on milling time and solution acidity. For solutions with natural acidity, the minimum copper concentrations were higher than 2.34 g/L across all milling times of carbon steel chips, consistently reached at 30 min of reaction. However, for carbon steel powders obtained after 10 and 15 h of milling, the minimum concentrations ranged from 0.69 to 0.71 g/L, achieved within 2 min of reaction. For powders obtained after 20 h of milling, the minimum copper ion concentrations were of 0.88 and 0.81 g/L, reached at 4 min and 2 min of reaction for 4.7 and 9.4 g/L sulfuric acid, respectively.

Table 1
Relevant parameters of the galvanic copper deposition influenced by the solution acidity and the milling of carbon steel chips.

Solution acidity, g/L	$C_{Cu,min}$, g/L	$t_{Cu,min}$, min	C_{Cu} (t = 30 min), g/L	C_{Fe} ($t_{Cu,min}$), g/L	η_{max}, %
Carbon steel chips					
0.0 g/L H_2SO_4	0.69	30	0.691	2.39	82
4.7 g/L H_2SO_4	0.60	30	0.60	2.71	84
9.4 g/L H_2SO_4	0.53	30	0.53	2.89	86
Carbon steel powders obtained at 10 h of milling					
0.0 g/L H_2SO_4	2.34	30	2.34	1.02	38
4.7 g/L H_2SO_4	0.71	2	2.33	2.89	81
9.4 g/L H_2SO_4	0.71	2	2.53	2.86	81
Carbon steel powders obtained at 15 h of milling					
0.0 g/L H_2SO_4	2.90	30	2.90	0.71	23
4.7 g/L H_2SO_4	0.69	2	2.35	2.81	82
9.4 g/L H_2SO_4	0.69	2	2.91	2.75	82
Carbon steel powders obtained at 20 h of milling					
0.0 g/L H_2SO_4	3.54	30	3.54	0.06	6
4.7 g/L H_2SO_4	0.88	4	2.48	2.71	77
9.4 g/L H_2SO_4	0.81	2	2.77	2.37	78

Regarding efficiencies, it can be observed that reaction times were significantly reduced when the galvanic copper deposition process was performed using carbon steel powders, saving up to 15 times the necessary time when using carbon steel chips. Additionally, solution acidity had a strong influence when using steel powders; however, for solutions with sulfuric acid concentration greater than 4.7 g/L, the efficiencies did not show significant changes. Under these conditions, milling carbon steel chips into powders for up to 10 h achieved similar efficiencies of 81 %–82 %. The changes in iron ion concentration are in concordance with the maximum efficiencies and copper ion concentrations and are related to the electrochemical reactions involved in the galvanic process. Furthermore, the results indicate that the use of carbon steel powders in galvanic copper deposition is not advantageous in solutions of natural acidity (0.0 g/L H_2SO_4), where efficiencies lower than 38 % were reached.

3.3. Morphological analysis of deposited copper powders

3.3.1. Copper deposition using carbon steel chips

Morphological examinations of copper deposited on carbon steel chips during the galvanic process after 30 min of reaction are shown in Fig. 5. Under these conditions, the results indicate that the chips were fully covered by a copper layer, following similar morphological patterns to their initial shape (Fig. 5a), along with preferential zones where a high copper content was observed. This was seen in both natural and variable acidity, showing a similar trend to that observed for Asadrokht and Zakeri [7] in the galvanic Al|Cu couple. The growth of this copper layer aligns with the kinetic tendency observed in Fig. 3, which are associated with a reduction in active sites for the iron oxidation reaction. In the results, most of the copper particles exhibited granular or multi-angular growth, with densely packed domains and well-defined borders delimiting the formation of agglomerates. Notably, solution acidity had a significant effect on the deposited copper morphology, showing a preference for forming individual copper particles rather than agglomerates. In the solution with natural acidity, individual copper particles with average sizes smaller than 2 μm were observed (Fig. 5b). In contrast, solutions with variable acidity showed copper agglomerates with average sizes around 10 μm (Fig. 5c–d). Under these last conditions, the size of individual copper particles trends to decreases with increasing the solution acidity (Fig. 5d).

3.3.2. Copper deposition using carbon steel powders

SEM images of the morphological patters of copper deposited on carbon steel powders are shown in Fig. 6 at different solution acidities after 30 min of reaction. The morphological patterns for experiments with a solution of natural acidity (0,0 g/L H_2SO_4) (Fig. 6a–c) displayed

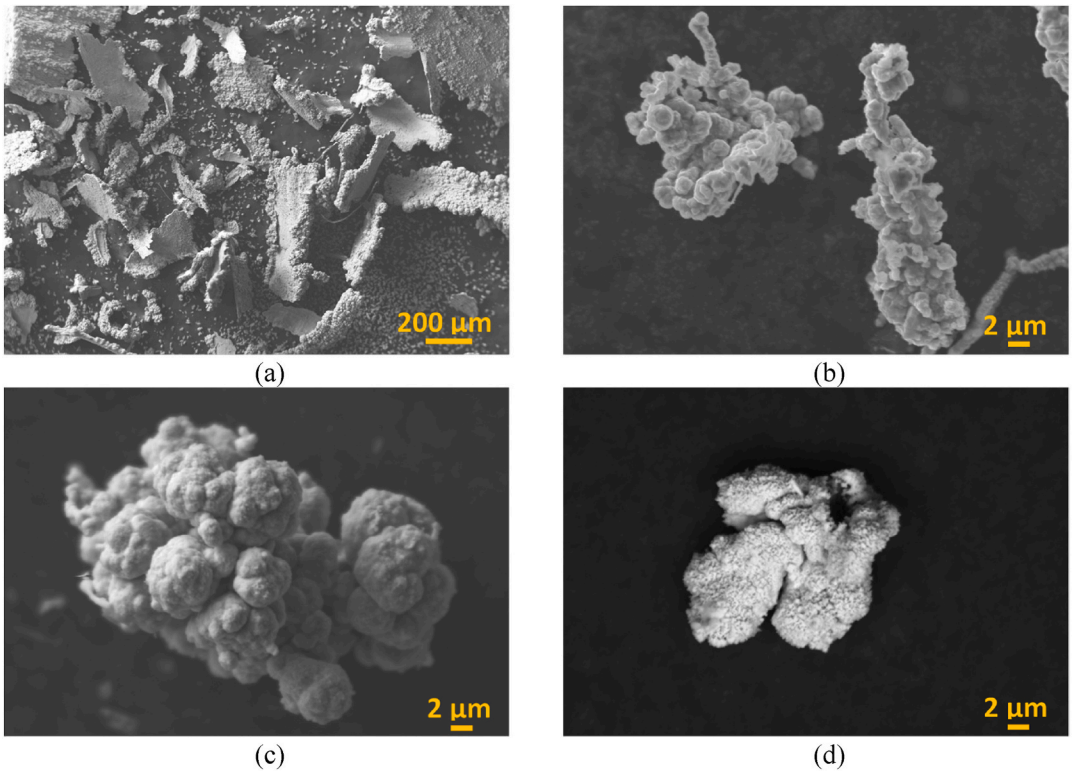


Fig. 5. SEM images of copper deposited on carbon steel chips after galvanic process in solutions of (a, b) natural acidity, (c) with an additional 4.7 g/L H_2SO_4, and (d) with an additional 9.4 g/L H_2SO_4.

the formation of dispersed crystal with multi-angular geometry, which also formed agglomerates ranging in size up to 10 µm for 10 and 15 h of milling. However, as the milling time increased from 10 to 20 h (Fig. 6c), the results revealed larger agglomerates of approximately 35 µm in diameter. This evidence supports the formation of turbulent agglomerates due to hydrodynamic behavior, observed in particles with sizes smaller than 10 µm, such as those obtained after 20 h of milling. This finding is concordant with the chemical and physical synergism mechanism, which promotes the encapsulation of carbon steel powders by a copper film deposited on the external surface of the agglomerates which is responsible for the limited galvanic copper deposition rate, mainly for the results using carbon steel powders milled during 10 h as seen in the results of Fig. 4a.

Fig. 7 presents metallographic images with EDS analysis, clearly showing the carbon steel matrix covered by a metallic copper film, which limits the galvanic deposition process. This confirms relevant aspects related to the low galvanic copper deposition rate, specifically the encapsulation of carbon steel powders by a copper film around this.

The morphological patterns of deposited copper on carbon steel powders for solutions with variable acidity are shown in Fig. 6d–i. These results do not reveals appreciable changes in the morphological patterns for any milling time, where, in general, a granular morphology is observed in all cases with similar agglomerate sizes. However, unlike the results observed in the experiments using carbon steel chips or solutions with natural acidity, these results show significant breakdown of the agglomerates, resulting in foam-like patterns with varying pore morphologies (see yellow ▲ symbols in Fig. 6). These changes can be attributed to the hydrogen evolution reaction thought the $Cu|H_2$ galvanic couple at longer reaction times ($t > 15$ min, as shown in Fig. 4), where the evolved hydrogen bubbles, visually observed during the experiments, promotes the breakdown of the previously deposited copper layer by increasing pressure inside or at the borders of the agglomerates. This, in turn, enhances the release of encapsulated carbon steel particles for their further oxidation. The formation of this pores was also observed by Djokić [44] during copper cementation using aluminum, where hydrogen evolution occurred through the water reduction reaction. Additionally, the copper particle sizes were found smaller than 0.7 µm, which were detached from the breakdown of the agglomerates.

3.4. Characterization and chemical analysis of deposited copper

The copper deposited on the carbon steel samples was scanned in the range of $10^\circ \leq 2\theta \leq 70^\circ$. Fig. 8 shows prominent peaks associated to crystalline structure of copper in their different planes as the main phase. Additionally, very weak peak associated with a ferrite phase accompany the copper peaks, indicating the presence of unreacted carbon steel powders. A similar situation was observed for all cases in solution with variable acidity. In contrast, the XRD patterns obtained by using carbon steel powders in a solution with natural acidity revealed high-intensity peaks corresponding to ferritic and iron oxide phases as goethite (α-FeOOH) and $Fe(OH)_2$, as well as cooper oxides, indicating a limited or absent galvanic copper deposition process. These results are in concordance with the temporal copper and iron concentration profiles shown in Fig. 4a–c and e, and align with the morphological observations discussed in the Section 3.3.

The X-ray Rietveld refinement method was used to acquire microstructural parameters for copper after the galvanic process in 4.7 g/L H_2SO_4 at different milling times of carbon steel chips. The microstructural results reveal crystallite sizes of 72 ± 0.11, 70 ± 0.17 and 59.5 ± 0.10 nm and lattice microstrains of $3.8{\cdot}10^{-4}{\pm}2.25{\cdot}10^{-5}$, $5.2{\cdot}10^{-4}{\pm}1.12{\cdot}10^{-5}$ and $4.7{\cdot}10^{-4}{\pm}1.21{\cdot}10^{-5}$ for milling times of 10, 15 and 20 h, respectively. Additionally, lattice parameter values were $0.3618 \pm 3{\cdot}10^{-6}$, $0.3615 \pm 2{\cdot}10^{-5}$ and $0.3619 \pm 5{\cdot}10^{-6}$ nm for 10, 15 and 20 h of milling, respectively. No clear trends were observed for crystallite size and microstrain as a function of milling time, indicating that milling have minimal influence on the microstructural behavior of deposited copper during the galvanic process. Furthermore, the lattice parameter are in close agreement with theoretical lattice parameter for

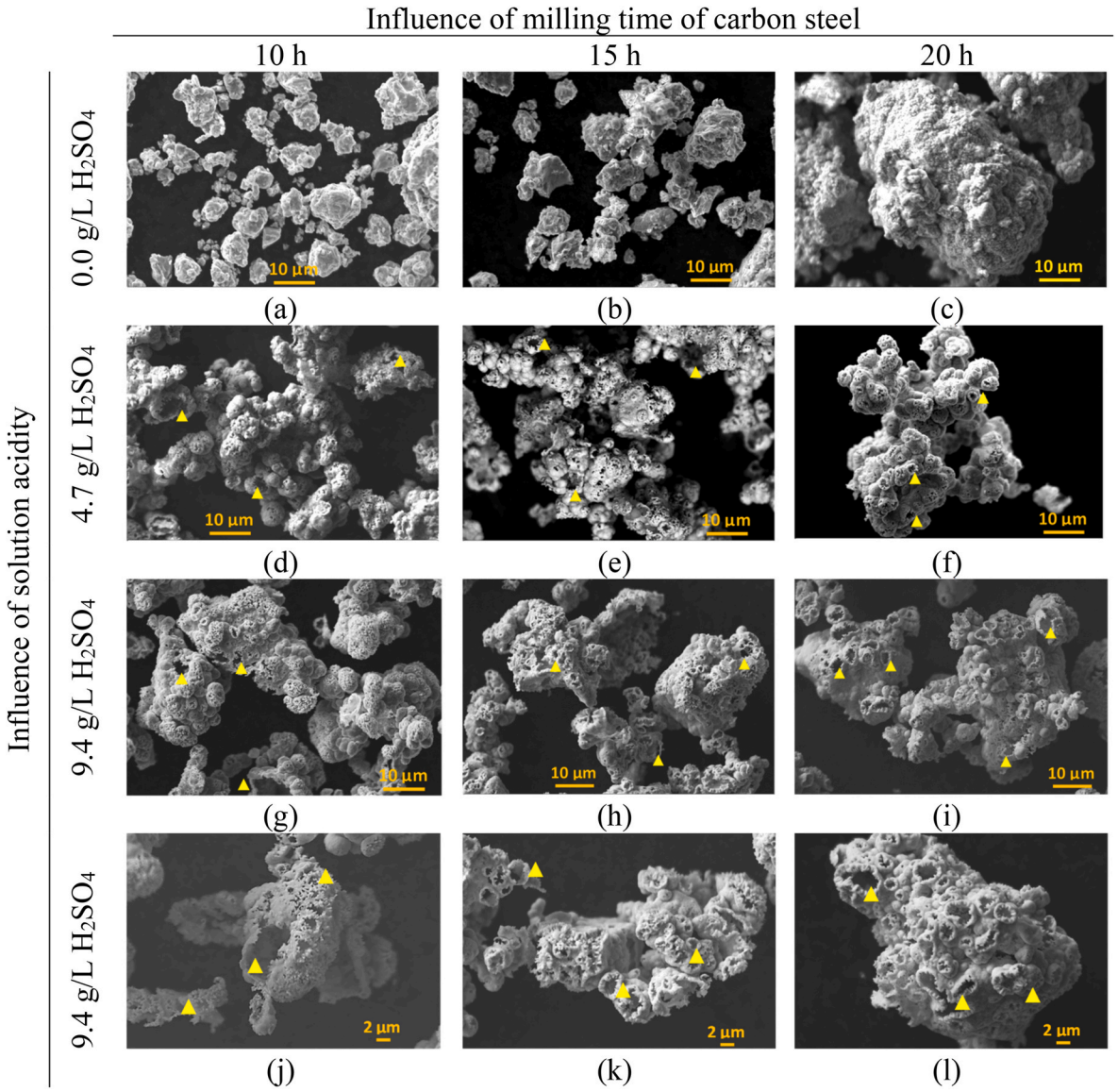


Fig. 6. SEM images of copper powders obtained after galvanic copper deposition under varying H_2SO_4 concentrations and different milling times of carbon steel chips. Yellow ▲ symbol denotes the position in where a breakdown of the agglomerated have been occurred.

copper (0.36147 nm) [45], suggesting negligible expansion or contraction of the unit cell volume during galvanic copper deposition. The averages reliability factors were Rwp(%) = 4.54, Rb(%) = 3.47, χ^2 = 1.77, Rexp(%) = 3.03.

Using a micro-Raman system, the copper powders obtained after galvanic deposition, were spectroscopically characterized by Raman spectroscopy. Additionally, the microscope integrated into the system allowed for capturing images of the samples. Representative spectra and images for the products obtained from copper galvanic deposition on carbon steel powders are shown in Fig. 9a–h. As observed in the images, metallic copper phase can be clearly identified when the copper deposition process was performed in acidic solution (4.7 g/L H_2SO_4) by using carbon steel powders prepared by milling during 10, 15 and 20 h. However, in the experience in natural media (0.0 g/L H_2SO_4) by using carbon steel milled during 20 h in, it is possible to observe homogeneous grains with brown and black color. Related to the Raman spectra, the unique sample that displays vibrational signals is the sample obtained using carbon steel powder prepared by 20 h of milling in natural media (Fig. 9h). This Raman spectrum exhibits several bands with varying relative intensities. The signals with the highest relative intensity are observed at 225 and 292 cm^{-1}. Three additional bands of medium relative intensity appear at 403, 501, 604 and 1302 cm^{-1}. Finally, a single band with very low relative intensity is observed at 549 cm^{-1}. The pattern of signals, in terms of both Raman shift and relative intensities, is consistent with the presence of goethite (α-FeOOH) and oolitic hematite [46]. Associated to the other samples obtained by using carbon steel powder in acidic solution, the absence of any Raman signals in each spectral profile indicates the presence of zero-valent copper, as metallic Cu does not exhibit Raman-active modes.

Furthermore, representative experimental conditions were selected to determine the copper grade in the deposited copper powders after the galvanic process. The results presented in Table 2 reveal a high purity grade of copper powders, ranging between 90 and 94 % for the experiments using carbon steel powders in solutions with variable acidity. This contrasts with the 39.6 % purity obtained when using carbon steel chips under similar solution acidities and residence time, due to the copper film covering the steel chips. The remaining chemical balance is associated with the iron content in the carbon steel particles that did not react during galvanic copper deposition, likely due to encapsulation of these particles as observed in Fig. 7. The copper grades obtained align

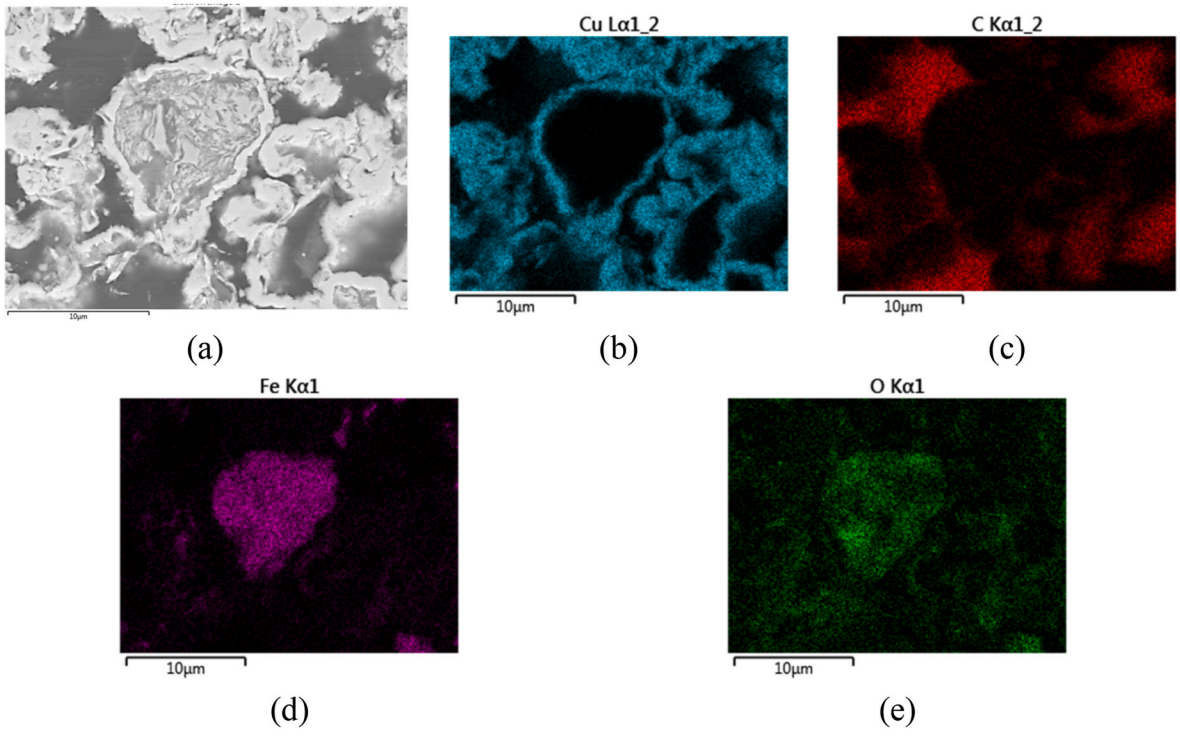


Fig. 7. SEM and EDS images of copper layer deposition on carbon steel powders.

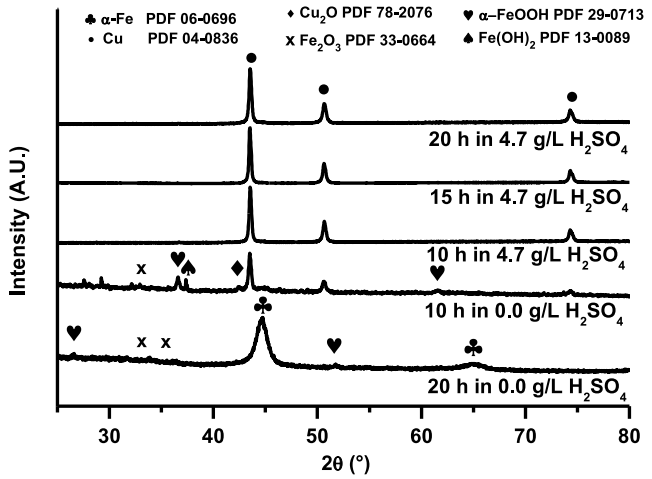


Fig. 8. XRD patterns of copper powders obtained after galvanic deposition using carbon steel powders prepared through high-energy ball milling for milling times of 10, 15 and 20 h, in solutions with and without addition sulfuric acid.

with the kinetic curves and morphological inspections, where a slight decrease in copper purity was observed with increased milling time.

3.5. Electrochemical results

Fig. 10 shows the temporal changes in the OCP of carbon steel powder samples under multiples conditions. For the galvanic process by using carbon steel powders in acid solution (4.7 g/L H_2SO_4), the OCP behavior display three well-defined regions. The region I is characterized by a negative shift in the OCP values, stabilizing around −280 mV/SHE. This region corresponds to a typical cementation process where the copper reduction reaction occurs via diffusion of copper ions from bulk solution to the cathodic sites on the carbon steel powders [47], establishing a mixed potential close to the thermodynamic equilibrium potential for the iron oxidation as shown in the Pourbaix diagram for Fe–H_2O system (see red ● symbol in Fig. S4a in the Supporting Information). Region II shows an exponential positive shift in the OCP values, reaching up to approximately 180 mV/SHE. This behavior is related to the depletion of active sites for iron oxidation on the carbon steel powders and the stabilization of the deposited copper particles. The potential range, between −280 and 180 mV/SHE, aligns with the stability region for solid copper in the Cu–H_2O Pourbaix diagram (see blue ● symbol in Fig. S4b in the Supporting Information). The region III is marked by a stable OCP values of approximately 218 mV/SHE. This potential is close to the thermodynamic equilibrium potential for the Cu|Cu^{+2} redox couple (see green ● symbol Fig. S4b in the Supporting Information), indicating that the previously deposited copper is beginning to undergo reoxidation. Here, the fact is supported by the copper ion concentration profile shown in Fig. 4 at times higher than 5 min, where the hydrogen evolution reaction acts as the cathodic counter-reaction that was also visually observed during the process. Furthermore, Fig. 10 indicates that the milling time has no significant influence on the OCP behavior of carbon steel in the sulfuric acid test solution, confirming that the galvanic copper deposition is reached at times of approximately 5 min. In contrast, OCP measurements for carbon steel powders in solutions with natural acidity show a nearly constant potential of 417 mV/SHE throughout the experiment. As previously discussed, under these conditions, the galvanic copper deposition is limited due to the formation of a passive film on the carbon steel powder surface. This observation is also supported by the XRD and Raman analysis presented in Figs. 8 and 9, respectively. In addition, the potential of 417 mV/SHE is in concordance with the thermodynamic stability of the Fe_2O_3 and FeOOH phases at pH 4.48, according to the Pourbaix diagram for Fe–H_2O system (see orange ● symbol Fig. S4a in the Supporting Information).

3.6. Kinetic model proposal

A kinetic model to describe the galvanic copper deposition using

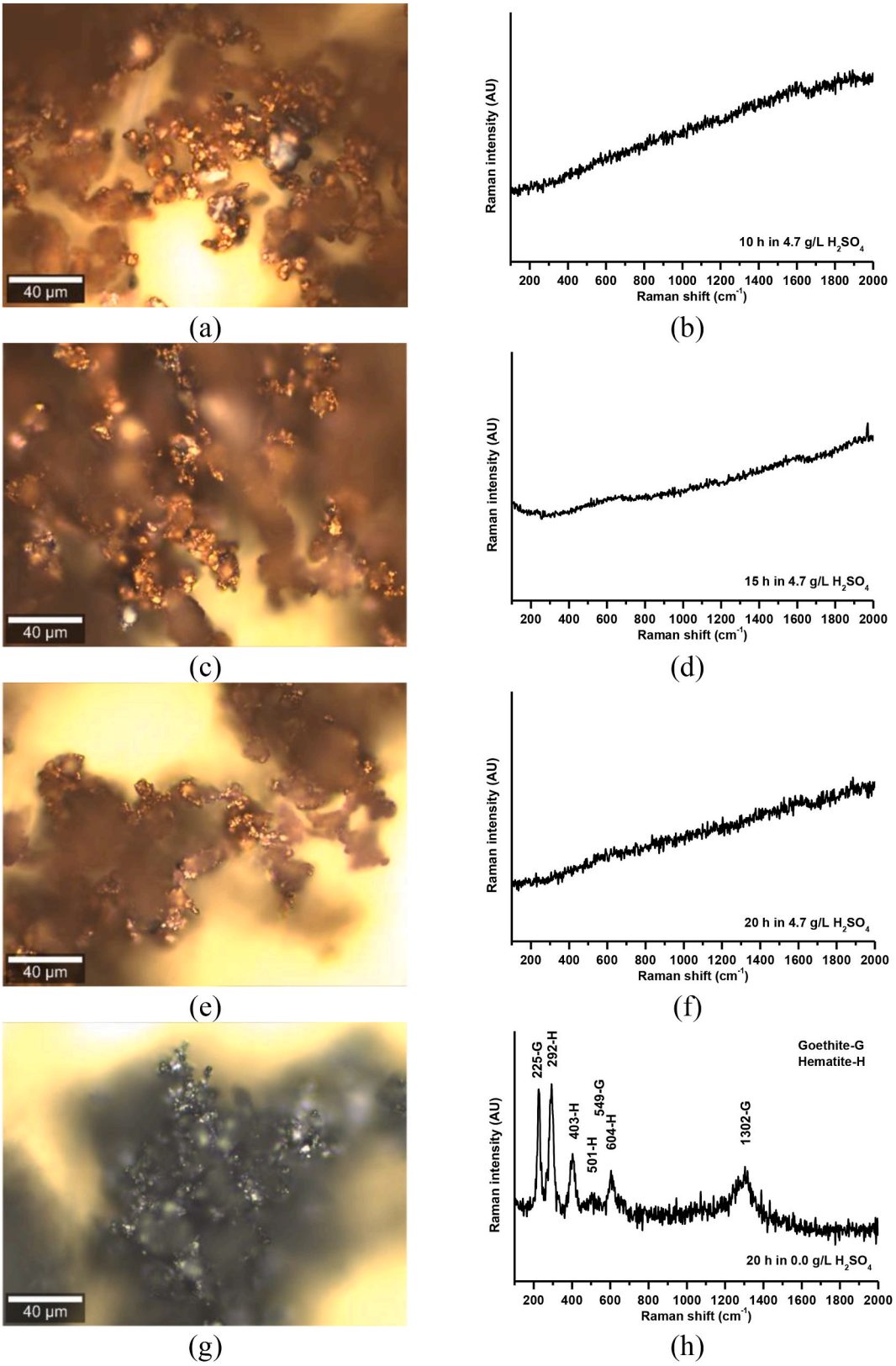


Fig. 9. Images and Raman spectra of copper powders obtained after galvanic deposition using carbon steel powders prepared through high-energy ball milling for milling times of (a and b) 10 h, (c and d) 15 h, (e and f) 20 h in solutions 4.7 g/L H_2SO_4, and (g and h) 20 h in 0.0 g/L H_2SO_4.

Table 2
Chemical analysis of cooper powder obtained after 10 min of galvanic deposition on carbon steel chips and powders.

Test solution	Carbon steel sample	Grade of copper in deposited powders (%)
4.7 g/L H_2SO_4	Chips	39.6
4.7 g/L H_2SO_4	Powders obtained during 10 h of milling	94.8
4.7 g/L H_2SO_4	Powders obtained during 15 h of milling	92.3
4.7 g/L H_2SO_4	Powders obtained during 20 h of milling	91.9

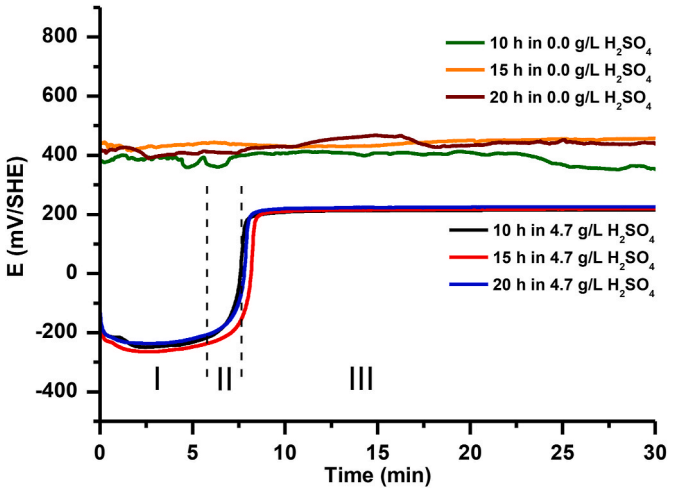


Fig. 10. OCP vs. time plot for galvanic copper cementation affected carbon steel milling time and solution acidity.

carbon steel chips and powders was developed by considering the temporal changes in copper and iron ion concentrations. Several studies have indicated that this process follows first-order kinetics [7,26,27,48,49]. However, other studies suggests that second-order kinetics can also describe this process [5]. Given the complexity of the results, which involves: i) the absence of reoxidation of previously deposited copper when using chips under any solution acidity conditions at longer times, ii) a lower copper deposition rate when using carbon steel powders in solutions of natural acidity, and iii) reoxidation of previously deposited copper in parallel with hydrogen evolution reaction at very short times, this study analyzed a kinetic model that describes the relationship between the copper and iron ion changes with time. The experimental data were fitted to a differential equation model that describes the kinetics of carbon steel chips and powders in acidic solution and natural pH solutions, following Equation (5) and Equation (6), which also incorporates a zero-order component to describe the oxidation of previously reduced copper during galvanic deposition. The assumption of a zero-order kinetics for the reoxidation of previously deposited copper is supported by the continuous increase in copper ion concentration and the constant iron ion concentration in solution, as shown in Fig. 4 of the experimental results, after the firsts 2 min of reaction.

$$\frac{dC_{Cu}}{dt} = -k_f \cdot C_{Cu} \cdot C_{Fe} + k_b \tag{5}$$

$$\frac{dC_{Fe}}{dt} = k_f \cdot C_{Cu} \cdot C_{Fe} \cdot (1-\alpha) \tag{6}$$

where, k_f and k_b are the kinetic constants for the forward copper reduction and the backward copper oxidation reaction, and α is a constant associated to the grade of the carbon steel surface coverage that limits the further iron oxidation reaction.

The date fitting was performed using the function ODE45 in MATLAB software. Fig. 11 shows examples of the experimental and fitted results for the temporal variations of copper and iron ions. These results clearly demonstrate a good fitting to the results confirming the proposed kinetics models. As presented in Table 3, for samples of carbon steel chips, the constants k_f increase with the sulfuric acid concentration in solution, in contrast to the α parameter, which decreases with increasing the solution acidity. These results are consistent with previous observations, where sulfuric acid promotes an increase in the reaction rate, favoring copper deposition, which also is associated with the reduction in α parameter indicating a major active surface on chips for the iron oxidation. Furthermore, a different trend was observed for carbon steel powders in solution of natural acidity. In this case, the constant k_f going to decreases as sulfuric acid concentration increase, indicating a decline in the galvanic process. This decline is associated to the variations in α constant, confirming a lower number of active sites available for the iron oxidation reaction, which can be associated to the formation of barriers as indicates XRD and Raman analysis through layers of Fe_2O_3, FeOOH, or the self-encapsulation for a cooper layer. The absence of the k_b constant indicates an irreversible reaction for copper deposition, as also is shown in Fig. 3.

On the other hand, the results tabulated in Table 4 clearly indicate that the k_f constant increases with solution acidity for the three studied milling times, thus promoting a rapid deposition process. Compared with results obtained for carbon steel chips in acid solutions, the kinetic constants for the results obtained by using carbon steel powders under similar conditions was approximately 23 times higher confirming a fast kinetic copper deposition process. On the other hand, the kinetic constant associated with copper reoxidation (k_b) does not show significant variations, suggesting it is independent of the studied solution acidity and milling times for carbon steel. The lower magnitude of the α parameter under these conditions indicates a high consumption rate of carbon steel powders during the iron oxidation reaction, which is also corroborated by XRD and Raman studies shown in Figs. 8 and 9. In summary, it can be indicated that for the galvanic copper deposition process is not recommendable to use carbon steel powders in copper solutions with natural acidity. In contrast, for solutions with variable acidity, using carbon steel powder obtained after 10 h of milling is a recommendable option to a fast copper deposition process, which is consistent with the observed reduction efficiencies.

4. Conclusions

This work investigated a novel approach for producing zero-valent copper powders via galvanic deposition, using carbon steel powders prepared by high energy ball-milling. We demonstrated that the milling time of carbon steel chips significantly influenced the copper deposition process, particularly when compared to the use of carbon steel chips, showing favorable and unfavorable behaviors depending on the acidity of the test solution. The key conclusions are as follows:

1) When using carbon steel chips, the copper deposition process was relatively slow, requiring residence times longer than 30 min and achieving efficiencies close to 82 %. These efficiencies were slightly increased with the addition of sulfuric acid to the solution.
2) The copper deposition process using carbon steel powders was significantly affected by the solution acidity, which played a crucial role. In solutions of natural acidity, longer milling times of carbon steel led to a decline in the galvanic reaction, attributed to the formation of a passivating barrier on the surface of the carbon steel particles, as corroborated by XRD and Raman analysis. In contrast, in acidic solutions, the reaction kinetics improved considerably, reducing reaction times to as little as 5 min and achieving efficiencies close to 80 %. However, longer residence times promoted the reoxidation of previously deposited copper, associated with the hydrogen

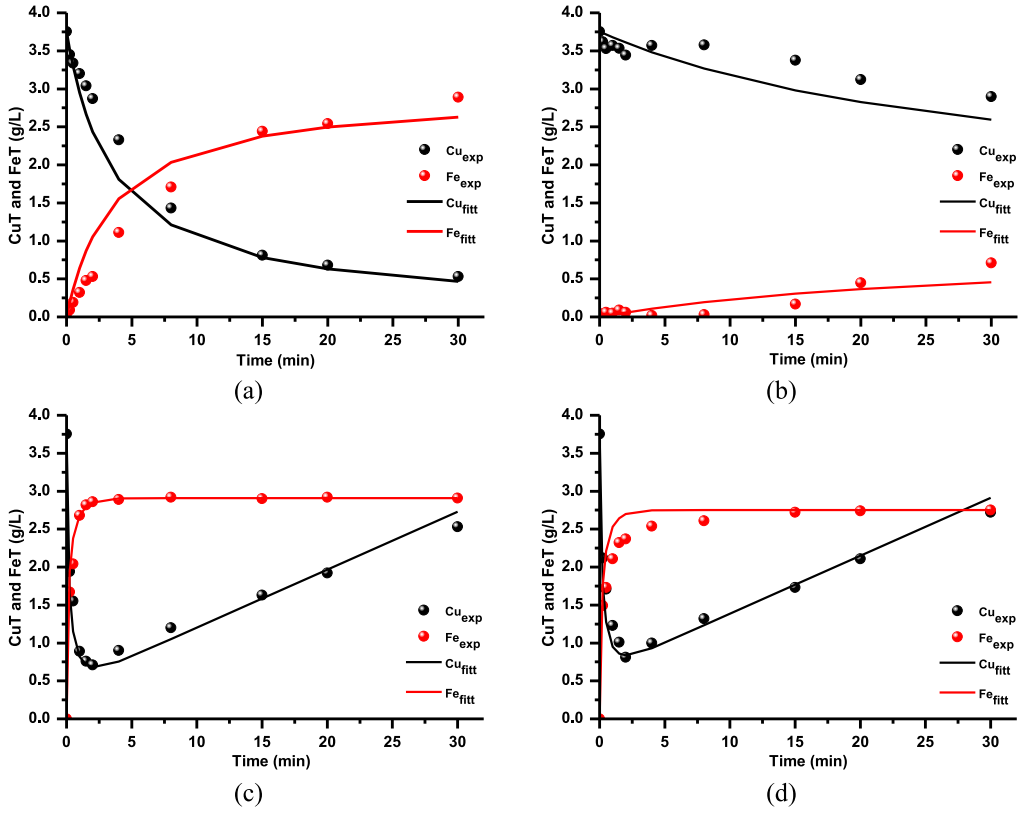


Fig. 11. Experimental and fitted kinetic curves for copper and iron ion concentrations during galvanic copper deposition for different conditions: a) carbon steel chips in 9.4 g/L H_2SO_4, b) carbon steel powders milled for 15 h of milling in 0.0 g/L H_2SO_4, c) carbon steel powders milled for 10 h in 9.4 g/L H_2SO_4, and d) carbon steel powders milled for 20 h in 9.4 g/L H_2SO_4.

Table 3
Effect of solution acidity on the kinetic parameters for galvanic copper deposition using carbon steel chips, and carbon steel powders in a solution of natural acidity. The fitting correlation is shown for the temporal profiles of copper and iron.

Additional sulfuric acid in solution, g/L	k, L/mol. min	α	R^2	
			Cu curve	Fe curve
Carbon steel chips				
0.0	4.2	0.20	0.99	0.97
4.7	4.7	0.10	0.98	0.94
9.4	5.3	0.09	0.98	0.96
	Milling of 10 h			
0.0	3.2	0.31	0.98	0.90
Milling of 15 h				
0.0	1.6	0.55	0.59	0.77
Milling of 20 h				
0.0	0.45	0.8	0.70	0.80

Table 4
Effect of solution acidity on the kinetic parameters for galvanic copper deposition using carbon steel powders, which were obtained through high-energy ball milling at 10, 15 and 20 h. The fitting correlation is shown for the temporal profiles of copper and iron.

Additional sulfuric acid in solution, g/L	kf, L/mol.min	kb, mol/L. min	α	R2	
				Cu curve	Fe curve
Milling of 10 h					
4.7	112	0.0011	0.003	0.99	0.98
9.4	120	0.0011	0.002	0.98	0.98
Milling of 15 h					
4.7	110	0.0011	0.002	0.99	0.99
9.4	151	0.0013	0.001	0.98	0.98
Milling of 20 h					
4.7	56	0.0011	0.002	0.99	0.99
9.4	105	0.0012	0.002	0.97	0.96

evolution reaction, leading to the breakdown of the copper deposited layer on the agglomerates and the release of encapsulated carbon steel particles.

3) The copper grade in the powders obtained after galvanic process using carbon steel powders as a reducing agent were between 90 and 94 %, which is favorable for copper recovery processes in acidic solutions obtaining a high purity product. This values were much higher than those found for carbon steel chips which were close to 39 %.
4) The shifting in the electrochemical mixed potential for the Fe|Cu redox couple were in concordance with thermodynamics, leads to the formation of iron oxide/hydroxides, metal copper, and hydrogen gas.
5) A second-order kinetics model respect to copper and iron ions was found to describe the copper deposition using carbon steel chips and powders, including an additional zero-order kinetic for copper reoxidation when carbon steel powders is used in acidic solutions.

The study focuses on leveraging the existing infrastructure of small and medium-scale mining and metallurgical operations, which often face challenges in accessing electrolysis processes due to the substantial capital expenses required for infrastructure and equipment. Our results demonstrated that the production of carbon steel powders via high-energy ball milling enables the recovery of high copper contents through galvanic precipitation in relatively short periods. At the industrial level, this process is particularly attractive, as it requires minimal capital investment, limited to basic equipment such as a stirrer

galvanic reactor, a ball-mill, and carbon steel chips that can be sourced from metal-mechanical industries. The novelty of this study lies in overcoming one of the main limitations in galvanic precipitation process using iron scrap, namely, the low copper recovery yields and low purities. However, certain technical challenges remain that represent opportunities for future improvement, such as optimizing agitation systems to minimize agglomerate formation in the final product and fine-tuning the kinetic control of the process without compromising the quality of the recovered copper.

CRediT authorship contribution statement

Alvaro Soliz: Conceptualization, Data curation, Formal analysis, Investigation, Methodology, Resources, Software, Supervision, Writing – original draft, Writing – review & editing. **Pia Rojas:** Investigation, Methodology, Writing – original draft. **Danny Guzman:** Conceptualization, Investigation, Methodology, Resources, Supervision. **Luis Cáceres:** Formal analysis, Software, Validation, Writing – review & editing. **Felipe M. Galleguillos-Madrid:** Data curation, Validation, Writing – review & editing. **Norman Toro:** Data curation, Software, Writing – review & editing. **Freddy Celis:** Data curation, Investigation, Validation, Writing – review & editing.

Data availability statement

The processed data are available from the corresponding author upon request.

Declaration of competing interest

The authors declare that they have no known competing financial interests or personal relationships that could have appeared to influence the work reported in this paper.

Acknowledgments

The authors would like to acknowledge to the Project DIUDA-22430 of the Universidad de Atacama and the project Fondo de Innovación para la Competitividad Regional-Atacama (FIC-R) BIP-40013608, and to project ANID+FONDEQUIP+EQM230067.

Appendix A. Supplementary data

Supplementary data to this article can be found online at https://doi.org/10.1016/j.jmrt.2025.04.300.

References

[1] Schlesinger M, King MJ, Sole KC, Davenport WG. Extractive metallurgy of copper. sixth ed. 2021. USA.
[2] Nekouei RK, Rashchi F, Joda NN. Effect of organic additives on synthesis of copper nano powders by pulsing electrolysis. Powder Technol 2013;237:554–61.
[3] Li G, Wang N, Wang Y, Yan Y. Synthesis and performance characterization of nano-copper by electrochemical deposition method based on coaxial electrode structure. J Iran Chem Soc 2023;20:839–48.
[4] Soliz A, Alfaro C, Cáceres L, Guzman D. Morphological characterization of copper deposited by electrolysis influenced by presence of chloride ions. Rev Mater 2021; 26:e12941.
[5] Granata G, Tsendorj U, Liu W, Tokoro C. Direct recovery of copper nanoparticles from leach pad drainage by surfactant-assisted cementation with iron powder. Colloids Surf A Physicochem Eng Asp 2019;580:123719.
[6] Jhajharia R, Jain D, Sengar A, Goyal A, Soni PR. Synthesis of copper powder by mechanically activated cementation. Powder Technol 2016;301:10–5.
[7] Asadrokht M, Zakeri A. Effect of concurrent ball milling on cementation reactions: the case of Cu-Al system. Miner Eng 2018;125:15–25.
[8] Karavasteva M. Kinetics and deposit morphology of copper cementation onto zinc, iron and aluminium. Hydrometallurgy 2005;76:149–52.
[9] Masnadi M, Yao N, Braidy N, Moores A. Cu(II) galvanic reduction and deposition onto iron nano- and microparticles: resulting morphologies and growth mechanisms. Langmuir 2015;31:789–98.
[10] Zhang QL, Yang ZM, Ding BJ, Lan XZ, Guo YJ. Preparation of copper nanoparticles by chemical reduction method using potassium borohydride. Trans Nonferrous Met Soc China 2010;20:s240–4.
[11] Dang TMD, Le TTT, Fribourg-Blanc E, Dang MC. Synthesis and optical properties of copper nanoparticles prepared by a chemical reduction method. Adv Nat Sci Nanosci Nanotechnol 2011;2:015009.
[12] Akhgar BN, Kavanlouei M, Kazemi H, Ghavidel S, Dardman S. Effect of synthesis routes on the microstructural properties of nano zero-valent metals of Fe and Cu synthesized from the industrial copper solvent extraction process. Mater Chem Phys 2023;302:127704.
[13] Martins TAG, Falconi IBA, Pavoski G, de Moraes VT, Baltazar MdG, Espinosa DCR. Green synthesis, characterization, and application of copper nanoparticles obtained from printed circuit boards to degrade mining surfactant by fenton process. J Environ Chem Eng 2021;9:106576.
[14] Letchumanan D, Sok SP, Ibrahim S, Nagoor NH, Arshad NM. Plant-based biosynthesis of copper/copper oxide nanoparticles: an update on their applications in biomedicine, mechanisms, and toxicity. Biomolecules 2021;11:564.
[15] Sarwar N, Humayoun UB, Kumar M, Zaidi SFA, Yoo JH, Ali N, Jeong DI, Lee JH, Yoon DH. Citric acid mediated green synthesis of copper nanoparticles using cinnamon bark extract and its multifaceted applications. J Clean Prod 2021;292: 125974.
[16] Shubhashree KR, Reddy R, Gangula AK, Nagananda GS, Badiya PK, Ramamurthy SS, Reddy N. Green synthesis of copper nanoparticles using aqueous extracts from Hyptis suaveolens (L). Mater Chem Phys 2022;280:125795.
[17] Tanwar S, Parauha YR, There Y, Dhoble SJ. Green synthesis-assisted copper nanoparticles using Aegle marmelos leaves extract: physical, optical, and antimicrobial properties. Luminescence 2023;1:1–10.
[18] Demirkiran N, Ekmekyapar A, Kunkul A, Baysar A. A kinetic study of copper cementation with zinc in aqueous solutions. Int J Miner Process 2007;82:80–5.
[19] Elzahaby MH, Nosier SA, Sedahmed GH, Fathalla AS, Abdel-Aziz MH, El-Gayar DA. Cementation of copper on zinc in an unsubmerged jet reactor. Can Metall Q 2023; 62:311–21.
[20] Lei Y, Hu X, Zhu C, Sun C, Xu Q, Cheng H, Zou X, Lu X. Mechanism of ultrasound-assisted copper cementation in zinc sulfate solution. Miner Eng 2023;202:108307.
[21] Zaabar A, Aitout R, Amoura D, Maizia R, Makhloufi L, Saidani B. Effect of nettle plant extract on the overconsumption diminution of zinc as sacrificial metal during cementation of copper. Miner Eng 2019;142:105933.
[22] Gros F, Baup S, Aurousseau M. Intensified recovery of copper in solution: cementation onto iron in fixed or fluidized bed under electromagnetic field. Chem Eng Process Process Intensif 2008;47:295–302.
[23] Djoudi W, Aissani-Benissad F, Bourouina-Bacha S. Optimization of copper cementation process by iron using central composite design experiments. Chem Eng J 2007;133:1–6.
[24] El-Batouti M. Removal of copper metal by cementation using a rotating iron cylinder. J Colloid Interface Sci 2005;283:123–9.
[25] Annamalai V, Murr LE. Influence of deposit morphology on the kinetics of copper cementation on pure iron. Hydrometallurgy 1979;4:57–82.
[26] Gros F, Baup S, Aurousseau M. Copper cementation on zinc and iron mixtures: Part 1: results on rotating disc electrode. Hydrometallurgy 2011;106:121–33.
[27] Nassef E, El-Taweel YA. Removal of copper from wastewater by cementation from simulated leach liquors. J Chem Eng Process Technol 2015;6:1000214.
[28] El-Saharty AA, El-Hammamy NH, El-Araby HA. Sodium diethyldithiocarbamate as accelerator of the rate of copper cementation. Egypt J Aquat Res 2015;41:289–93.
[29] Suryanarayana C. Mechanical alloying and milling. Prog Mater Sci 2001;46:1–184.
[30] Rao MD, Meshram A, Verma HR, Singh KK, Mankhand TR. Study to enhance cementation of impurities from zinc leach liquor by modifying the shape and size of zinc dust. Hydrometallurgy 2020;195:105352.
[31] Zhang J, Klasky M, Letellier BC. The aluminum chemistry and corrosion in alkaline solutions. J Nucl Mater 2009;384:175–89.
[32] Soliz A, Guzmán D, Cáceres L, Madrid FMG. Electrochemical kinetic analysis of carbon steel powders produced by high-energy ball milling. Metals 2022;12:665.
[33] Rietveld HM. A profile refinement method for nuclear and magnetic structures. J Appl Crystallogr 1969;2:65–71.
[34] Lutterotti L. MAUD—Materials analysis using diffraction. Available online: http://maud.radiographema.eu/. [Accessed 15 April 2024].
[35] Pearson WB. A handbook of lattice spacings and structures of metals and alloys, vol. 4; 1958. UK.
[36] Soliz A, Cáceres L. Corrosion behavior of carbon steel in LiBr in comparison to NaCl solutions under controlled hydrodynamic conditions. Int J Electrochem Sci 2015; 10:5673–93.
[37] Awaad IM, Nosier SA, Hussein M, Elnahrawy MS, Sedahmed GH, Abdel-Aziz MH, El-Naggar MA. Copper extraction from dilute solutions by cementation in a gas-sparged helical coil reactor. JOM 2022;74:963–70.
[38] Van den Berg J, Yang Y, Nauta H, Van Sandwijk A, Reuter M. Comprehensive processing of low grade sulphidic molybdenum ores. Miner Eng 2002;15:879–83.
[39] Roberge PR. Handbook of corrosion engineering. third ed. 2019. USA.
[40] Morgan B, Lahav O. The effect of pH on the kinetics of spontaneous Fe(II) oxidation by O_2 in aqueous solution–basic principles and a simple heuristic description. Chemosphere 2007;68:2080–4.
[41] Jolivet JP, Chanéac C, Tronc E. Iron oxide chemistry. From molecular clusters to extended solid networks. Chem Commun 2004;5:481–3.
[42] Sun Z, Yang L, Shen A, Zhou L, Wu H. Combined effect of chemical and turbulent agglomeration on improving the removal of fine particles by different coupling mode. Powder Technol 2019;344:242–50.

[43] Guo Q, Yang Z, Zhang J. Influence of a combined external field on the agglomeration of inhalable particles from a coal combustion plant. Powder Technol 2012;227:67–73.
[44] Djokić SS. Cementation of copper on aluminum in alkaline solutions. J Electrochem Soc 1996;143:1300.
[45] Simon NJ, Drexler ES, Reed RP. Properties of copper and copper alloys at cryogenic temperatures. Final report; materials science and engineering laboratory. Boulder. USA: National Institute of Standards and Technology; 1992.
[46] Marshall C, Stockdale G, Carr C. Raman spectroscopy of geological varieties of hematite of varying crystallinity and morphology. J Raman Spectrosc 2025;1.
[47] Tzaneva B, Petrova T, Hristov J, Fachikov L. Electrochemical investigation of cementation process. Bulg Chem Commun 2016;48:91–5.
[48] El-Ashtoukhy ES, Abdel-Aziz M. Removal of copper from aqueous solutions by cementation in a bubble column reactor fitted with horizontal screens. Int J Miner Process 2013;121:65.
[49] Miller JD, Beckstead LW. Surface deposit effects in the kinetics of copper cementation by iron. Metall Trans A 1973;4:1967–73.